View metadata, citation and similar papers at core.ac.uk

brought to you by CORE

provided by Loughborough University Institutional Repository

This item was submitted to Loughborough's Institutional Repository (https://dspace.lboro.ac.uk/) by the author and is made available under the following Creative Commons Licence conditions.

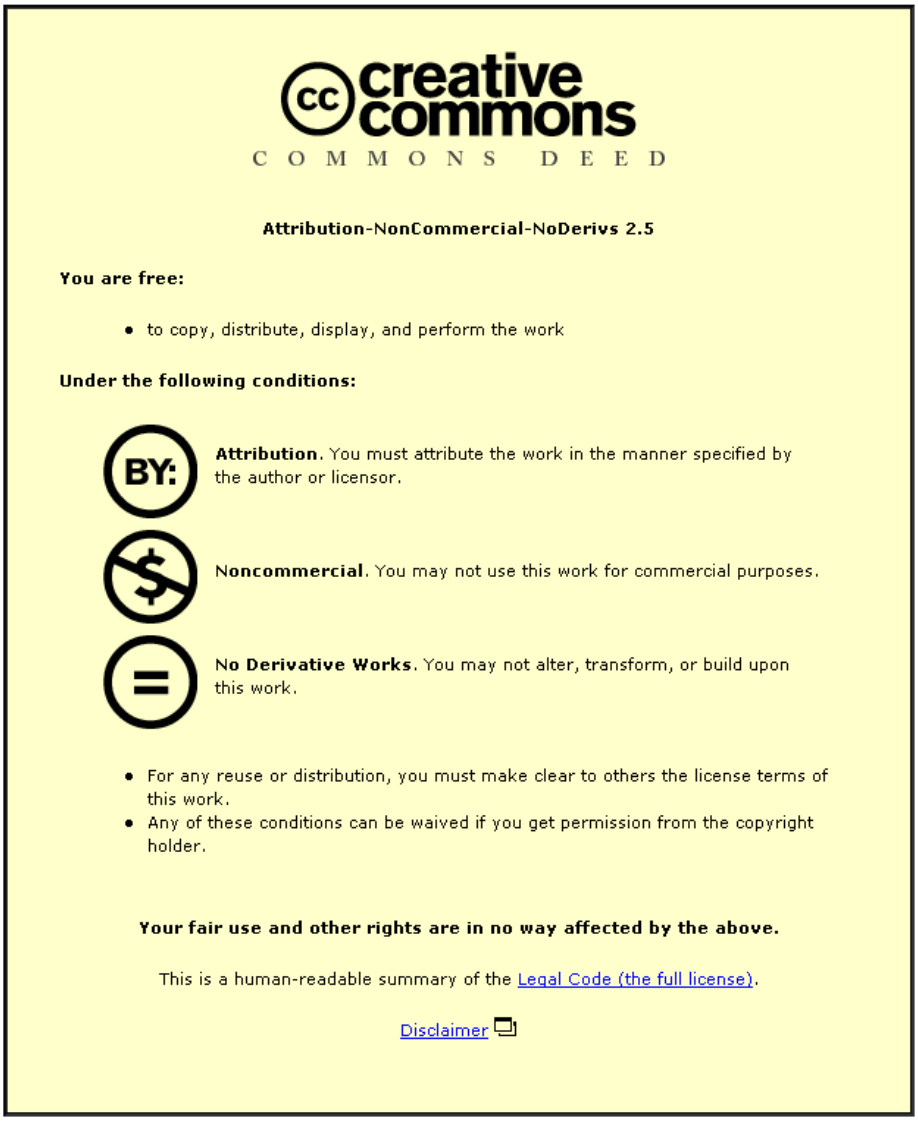

creative commons

COMMONS DEED

Attribution-NonCommercial-NoDerivs 2.5

You are free:

- to copy, distribute, display, and perform the work

Under the following conditions:

Attribution. You must attribute the work in the manner specified by the author or licensor.

Noncommercial. You may not use this work for commercial purposes.

No Derivative Works. You may not alter, transform, or build upon this work.

- For any reuse or distribution, you must make clear to others the license terms of this work.
- Any of these conditions can be waived if you get permission from the copyright holder.

Your fair use and other rights are in no way affected by the above.

This is a human-readable summary of the Legal Code (the full license).

Disclaimer

For the full text of this licence, please go to:
http://creativecommons.org/licenses/by-nc-nd/2.5/

Analysis of critical–length data from Electromigration failure studies

V.M. Dwyer

Department of Electronic and Electrical Engineering, Loughborough University, Loughborough, LE11 3TU, UK

Abstract

An accurate estimation of the Blech length, the critical line length below which interconnect lines are immortal, is vital as it allows EDA tools to reduce their workload. In lines longer than the Blech length, either a void will inevitably nucleate and grow until the line fails, or the line will rupture. The majority of failure analyses reveal voiding as the failure mechanism however recent analysis suggest Blech length failures are characterised by simultaneous [6] voiding and rupture, and a non-zero steady-state drift velocity. This paper provides an alternative interpretation of results.

1. Introduction

With the ongoing scaling of IC dimensions, copper interconnects become ever more susceptible to Electromigration (EM) failure. The more mobile metal atoms (typically those in the grain boundary network or at interfaces) are driven downstream by the high current density. In Dual Damascene (DD) copper, the line ends are terminated by a Ta–based barrier layer which prevents further progress. As a result the drifting copper is forced into the interconnect lattice, increasing compressive stresses close to the anode and tensile stresses close to the cathode. If sufficiently high, these stresses can lead to ruptures at the anode and voiding at the cathode, and either may cause interconnect failure.

A possible resource, in circuit design, is the critical length or Blech length effect. The stress gradient that builds up during copper migration leads to a back force which opposes the EM 'wind' force. In short lines a relatively small transfer of material is required to produce a gradient sufficient to offset the EM force, halt the metal migration, and so save the interconnect. Consequently all interconnect lines whose length L is shorter than some critical (Blech) length L_B are immortal as far as Electromigration failure is concerned. Either such lines are unable to generate sufficient stress to nucleate a void or, if they are able to nucleate a void, then both the line is unable to generate sufficient stress to cause the line to rupture *and* the line is unable to grow the void to a size sufficient for failure to occur. Using standard EM theory, based on the Stress Evolution Model (SEM) of Korhonen el al., the two former cases (nucleation and rupture) lead to critical values of the current density–length product jL [1], while the latter leads to a critical jL^2 [1, 2].

The word 'unable' in the present context means that, once the stress in the line reaches its steady-state, the tensile stress at the cathode ($x = L$) is too low for nucleation, $\sigma(L, t\rightarrow\infty) < \sigma_{cr}$; or the compressive stress at the anode ($x = 0$) is to too low to cause the line to rupture, $|\sigma(0, t\rightarrow\infty)| < |\sigma_{rup}|$, and the steady-state void volume is too small, $V(t\rightarrow\infty) < V_{cr}$, to cause the (typically 10%) increase in line resistance that indicates failure. For a given current density j, it will be the smaller of these critical lengths, for growth and for rupture (rather than their sum as suggested in [3]) that is expected to be the measured value for L_B.

For a theoretical line of length equal to the critical value, i.e. one with $L = L_B$, failure will occur only as the steady–state is reached, leading to an asymptotic failure

time $t_f \to \infty$. Similarly, all lines of length $L > L_B$ will fail in finite time and all lines of length $L < L_B$ will survive indefinitely. From this it is clear that the definition of L_B is the longest interconnect that does not exceed either the void or rupture thresholds before the steady–state condition in the line is reached. In the case of most lines it is voiding, rather than rupture, which causes the final failure; which implies that in most cases the rupture threshold is relatively high.

The situation differs slightly between passivated and unpassivated lines. For unpassivated lines, such as those of Blech's original gold on molybdenum experiments [4], there is no confinement to cause the compressive stress at the anode and the tensile stress at the cathode to rise with each transported atom. In such lines, the stress at the line ends builds up to steady–state levels, say $\sigma_C(\infty)$ and $\sigma_A(\infty)$, at the cathode and the anode respectively. If those stresses can generate a large enough gradient to balance the electron wind force, then EM will cease. If they are not, gold will continue to be displaced from cathode to anode. For an unpassivated line, in the steady–state, the gold ends will move at a steady velocity along the molybdenum. As the steady–state stress gradient, $(\sigma_C(\infty)-\sigma_A(\infty))/L$, is larger in shorter lines, a sufficiently short line can prevent electromigration, while longer lines cannot.

For the passivated lines used in ICs, the void front of a cathode void should not move in the steady–state, since that would imply atoms moving, stress redistribution, and a state not yet steady (the only exception to this is a steady rupture, considered later). Provided that this steady–state sets up before the various thresholds are reached, EM failure can be prevented. This is known as the short line effect, and can be vital in Electromigration–aware chip design as, by daisy chaining long interconnects, say in M1 and M2 sections, all lines can conceivably be made sufficiently short that EM ceases, this defines a critical or Blech length. In recent years a number of studies of the short line effect in DD copper have been reported [3, 5–14] some of which have indeed daisy chained interconnects of different lengths to increase the efficiency of the experiment. The purpose of this paper is to analyse that work using what might be described as standard theory for Electromigration [1].

Failure in copper interconnect begins with the nucleation of a void which is generally assumed to occur relatively quickly, although copper reservoirs and a variety of other techniques can slow this process down. For present purposes we shall assume that the voiding occurs at the cathode via [15]. Although there is much evidence that in a significant number of cases nucleation occurs several microns from the via, to which the void then drifts, such transient issues are unimportant here as it is asymptotic failure which is of interest.

Once the void is nucleated, the tensile stress at its free surface collapses, creating stress gradients close by which temporarily reinforce rather than oppose the EM force, sweeping neighbouring vacancies in the void [16]. After a period of initial relatively fast growth driven by this release of strain energy, the stress gradient force gradually dies out leaving only the EM wind force, which is independent of line length L [16]. The void then undergoes a period of reasonably constant growth.

For a line of length just below L_B, the growth rate will gradually decrease, as the stress gradient is re-established, until a new steady–state obtained. At $L = L_B$, just as the steady–state is set up, either the void volume, or the compressive anode stress, will reach the the critical void volume V_{cr}, or the rupture threshold σ_{rup}, asymptotically [1,2].

The atomic drift velocity v_{drift}, from Blech [4], is

$$v_{drift}(x,t) = \frac{D_a \Omega}{kT}\left(\frac{Z^* q \rho j}{\Omega} - \frac{\partial \sigma}{\partial x}\right) \qquad (1)$$

where D_a is the atomic diffusivity, Z^* the effective valence, ρ the copper resistivity, j the applied current density, Ω the atomic volume, kT the thermal energy and σ the tensile stress, (it will also be useful later to define the parameter $G = Z^* q \rho j/\Omega$). Averaging over the line length L, and setting $\Delta\sigma(t) = \sigma_C(t) - \sigma_A(t)$ to be the stress drop along the line, then gives

$$\bar{v}_{drift}(t) = \frac{D_a \Omega}{kT}\left(\frac{Z^* q \rho}{\Omega} j - \frac{\Delta\sigma(t)}{L}\right) \qquad (2)$$

For an unpassivated line, the steady–state occurs when the cathode and anode reach their final values and, in general, $\bar{v}_{drift}(t \to \infty) \neq 0$.

This case, which is valid for unpassivated lines [4], has also been used consistently in the case of passivated lines [3, 5–14]. In passivated lines, unless the anode is steadily leaking copper into the surrounding dielectric stack, the steady–state occurs only when $\bar{v}_{drift} = 0$. From eqn (1), this corresponds to $\sigma_{SS}(x) = \sigma_0 - Gx$ where the constant σ_0 depends upon the line boundary conditions, Fig (1).

In references [3,5–14] it is assumed that a rupture pins the anode stress at σ_{rup}. Should that happen the void will continue to grow until the flux leaking into the dielectric stack can be brought to a halt; this can only

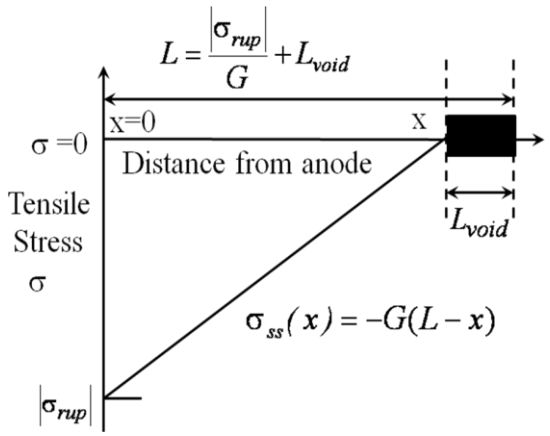

Fig. 1. The steady–state stress distribution for a line with a rupture, if the anode stress is pinned at σ_{rup}.

happen when the line length from the anode edge of the void to the anode is$|\sigma_{rup}|/G$, as shown in Fig. (1). If the line is not to fail, the void must also be less that the critical length $L_{void} = V_{cr}/A$, where A is the line cross–sectional area, and consequently the Blech length would becomes $L_B = |\sigma_{rup}|/G + L_{void}. \approx |\sigma_{rup}|/G$, i.e. the rupture threshold. If lines are rupturing, this indicates that this should be used to define the Blech length.

In references [11, 13, 14] only void growth is considered, although a critical value of the jL product (implying nucleation or rupture) is sought rather than jL^2, which is relevant to void growth [2]. References [5–8] define a probability of line failure, after the line ruptures and in the passivated case, as the ratio of two non–zero steady–state drift velocities,

$$P(j,L) = C\frac{\bar{v}_{drift}\{j,L\}}{\bar{v}_{drift}\{j,L_M\}} \qquad (3)$$

where the braces indicate the dependence of $\bar{v}_{drift}$ on the current density j and line length L, L_M is the longest line in the sample and C is a constant. Other authors [3, 9–14] associate the median time to failure $MTTF$ with

$$MTTF = \frac{L}{\bar{v}_{drift}\{j,L\}} \qquad (4)$$

The implications of eqns (3) or (4) are that the failure time is dominated by the time after a rupture, as it is only then when $\bar{v}_{drift} \neq 0$ is possible at steady–state, and further that the rupture occurs in the manner of a controlled overflow of atoms into the dielectric stack, leading to $\bar{v}_{drift}$ = constant, rather than as an unpredictable breach. A line that ruptures with a non–zero steady–state velocity $\bar{v}_{drift}$ *must* eventually fail, and for such lines the rupture condition must then determine the critical length. If the rupture pins the stress at the anode to a value lower than the rupture threshold $|\sigma_A| \leq |\sigma_{rup}|$, then the void growth rate will simply decrease the failure time compared to a more robust line.

The motivation behind eqns (3) and (4) is the assumption that the steady–state stress is created very quickly (which would also include the rupture at the anode), and following which the void grows according to eqn (2). This seems difficult to justify as it is also eqn (2) that is responsible for the atomic transport which sets up that steady–state. The original experimental results, on which this assumption is based, come from the work of Hu et al. [18–20 and references therein]. That work, however, refers to Al(Cu) interconnect which is generally characterised rather differently: by a long nucleation period and a shorter growth period, (n ~ 2 in the Black equation). In addition the steady–state so described relates to the migration of the Cu solute [18], prior to aluminium migration, and on the impact of the resulting stress profile on the aluminium drift. The activation energy for Cu diffusion in the Al(Cu) grain boundary network is considerably smaller that for the Cu–nitride interface [21, 22], consequently the time for the steady–state Cu profile to develop in Al(Cu) cannot be assumed to be representative of events in DD Cu. The analysis given in refs [18–20] is also only relevant to long interconnects [20], and consequently is unsuitable for analysis of the short length effect.

Within the current picture, any variation between samples in the void growth rate just after their nucleation is determined not by the length, but rather by variations in the EM part of the drift velocity $v_{drift}(x,t)$, i.e., essentially by variations between samples of the product Z^*D_a. Thus potentially this variation is caused by the same mechanism that causes variations in interconnect failure times. For lines close to the Blech length, the anode stress affects the growth rate, which will eventually drop to zero if the line does not fail first. For very long lines, however, the anode will have little impact and the void will grow large enough to cause failure. For large L, the growth rate is roughly constant, due to the roughly constant EM wind force, thus

$$t_f = \frac{V_{cr}}{v_{EM}(L)hw} = \frac{kTV_{cr}}{Z^*D_a q\rho jhw} \qquad (5)$$

The distribution of t_f is then dependent on the distributions of both the volume of copper moved V_{cr} and on the effective line diffusivity. In references [3, 5–14], and in most analysis V_{cr} is assumed fixed which for

now we do also. Bu contrast in lines close to L_B, it is clearly vital to also include the effects of the anode stress, which we do now.

2. Interpreting Blech length data

2.1. Nucleation/rupture experiments[5-8] $(jL)_{cr}$

Using a simple, one–dimensional linearised version of the stress evolution model (SEM) of Korhonen et al. [1], failure occurs when [e.g. 17]

$$\frac{(jL)_{cr}}{jL} = 1 - \frac{8}{\pi^2}\sum_{n=0}^{\infty}\frac{exp\left(-\frac{(2n+1)^2\pi^2\kappa t_f}{4L^2}\right)}{(2n+1)^2} \equiv g\left(\frac{\kappa t_f}{L^2}\right) \quad (6)$$

which also defines the function $g(\eta)$ in an obvious manner. κ is an effective diffusivity given by $\kappa = B\Omega D_a\delta_I/hkT$ for bulk modulus B, interface thickness δ_I and line height h. The critical value $(jL)_{cr}$ is given by $\Omega\Delta\sigma_{cr}/Z^*q\rho$ and independent of κ. When $jL \to (jL)_{cr}$ it is clear that $t_f \to \infty$, as expected. In terms of the dimensionless parameter $r = (jL)_{cr}/jL$, the failure time is

$$t_f = \frac{(jL)_{cr}^2}{j^2\kappa}\frac{g^{-1}(r)}{r^2} \quad (7)$$

where $\eta = g^{-1}(r)$ is the inverse function of $r = g(\eta)$. Note as, for fixed L, $g^{-1}(r)/r^2$ depends on j this is more complex than Black's equation. Since some of the rupture times are expected to be very long, some will be scheduled after the experiment has finished (at $t = t_{ex}$), whatever the value of t_{ex}. Such line lengths L will appear to be in a grey area; some mortal, some appearing immortal. The probability of immortality, within the lifetime of the experiment, which is sought by eqn (3), is then simply $P(j, L) = \Pr\{t_f > t_{ex}\}$ or equivalently $\Pr\{\kappa < (jL)_{cr}^2 g^{-1}(r)/j^2r^2t_{ex}\}$, from eqn (7). If the effective diffusivity values κ are distributed with a Cumulative Distribution Function (cdf) $F(\kappa)$ we obtain

$$P(j,L) = F\left(\frac{(jL)_{cr}^2 g^{-1}(r)}{j^2r^2t_{ex}}\right) \quad (8)$$

$P(j,L)$ now gives an important measure of the diffusivity cdf, as in Fig. 2. For lognormal D_a, and hence κ values (consistent with lognormal failure times in eqns (5) and (7)), with a median value of κ_{50} and lognormal standard deviation σ_{SD}, eqn (8) becomes

$$P(j,L) = \frac{1}{2} + \frac{1}{2}\mathrm{erf}\left(\ln\left(\frac{(jL)_{cr}^2 g^{-1}(r)}{j^2r^2\kappa_{50}t_{ex}}\right)\Big/\sqrt{2\sigma_{SD}^2}\right) \quad (9)$$

2.2. Growth time experiments [9–14] (jL^2)

The growth of a void, again using the SEM

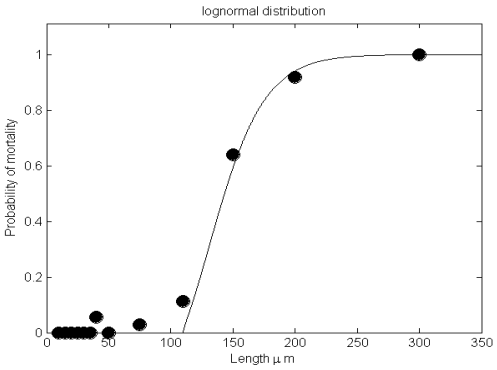

Fig. 2. Lognormal fit to data from ref [7,8].

equation of Korhonen et al. [1], follows the expression of He et al. [2], and failure occurs under the condition

$$\frac{(jL^2)_g}{jL^2} = 1 - \frac{32}{\pi^3}\sum_{n=0}^{\infty}\frac{exp\left(-\frac{(2n+1)^2\pi^2\kappa t_f}{4L^2}\right)}{(2n+1)^3} \equiv h\left(\frac{\kappa t_f}{L^2}\right) \quad (10)$$

where $(jL^2)_g = 2\Omega BV_{cr}/Z^*q\rho A$ is also independent of κ. This leads to failure time (again more complex than Black's) of

$$t_f = \frac{(jL^2)_g}{j\kappa}\frac{h^{-1}(s)}{s} \quad (11)$$

where s is the dimensionless parameter $(jL^2)_g/jL^2$, and $\xi = h^{-1}(s)$ is the inverse function of $s = h(\xi)$. If rupture is unlikely then, eqn (11) rather than eqn (7) should be used to fit the data in Fig. (2). In this case $P(j,L)$ is

$$P(j,L) = F\left(\frac{(jL^2)_g}{jt_{ex}}\frac{h^{-1}(s)}{s}\right) \quad (12)$$

References [3,9–14] also consider the dependence of $L/MTTF$ on jL. If D_a is lognormally distributed, eqns (7) and (11) imply that both t_f and L/t_f will also be so. Then from eqn (11) the median time to failure $MTTF$ is

$$\frac{L}{MTTF} = jL\frac{\kappa_{50}}{(jL^2)_g}\frac{s}{h^{-1}(s)} \quad (13)$$

since s is independent of κ. These authors also find an increasing value of the lognormal standard deviation for shorter lines. However, from say eqn (11),

$$log(t_f) = log\left(\frac{1}{jD_a}\right) + log\left(\frac{(jL^2)_g h^{-1}(s)/s}{\delta_I B\Omega/kTh}\right) \quad (14)$$

Clearly, from eqn (14), the effect of changing either j or L does not change σ_{SD}. A growing number of recent results, relating to in–line nucleation, void drift and extrusion occurrence, appear to show that accounting

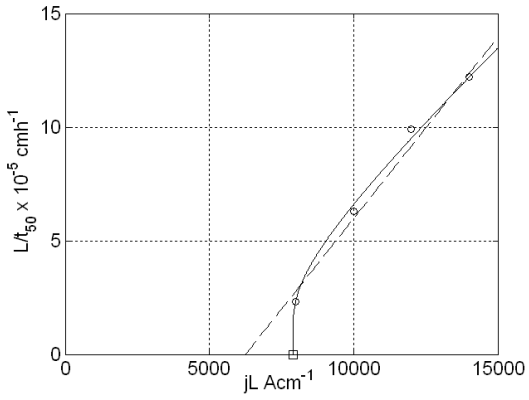

Fig. 3. Estimating L_{cr} using data from ref [11].

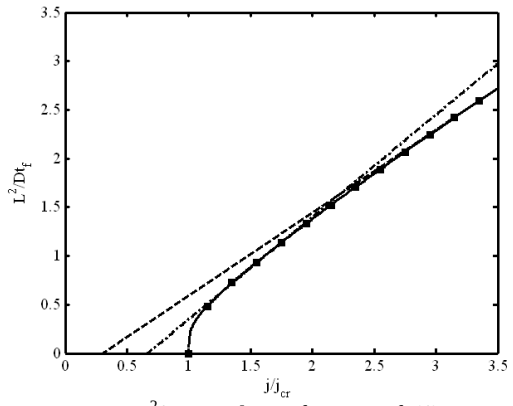

Fig. 4. Fitting L^2/Dt_f to a linear function of j/j_{cr}

for variations in D_a with individual grain orientations, is necessary to interpret EM effects [17]. Consequently, short lines with fewer grains will have a wider variation. In other words, the analysis above should probably include intra–grain variations in D_a. This may then explain the increase in the variation σ_{SD} as L decreases.

3. Results

Using eqns (8) and (12), it is now a simple matter to reinterpret the results of references [3, 5–14].

3.1. Nucleation/Rupture time experiments [5–8] (jL)

Fig. (2) shows a comparison of results taken from references [7, 8] with theoretical results from eqn (9). The distribution of D_a values is assumed to be lognormal with a median value D_{a50} and a lognormal deviation σ_{SD}. The fit corresponds to σ_{SD} = 0.7 and $\kappa_{50}t_{ex}/L_{cr}^2$ = 0.2. As t_{ex} was 45 days in the experiment, and L_{cr} ~ 110 μm [7,8], i.e. κ_{50} ~ 9.3×10^{-16} m^2/s. If $B\Omega/kT$ ~ 40 [17] this gives a median effective atomic diffusivity of $D_{eff,50} = \delta_I D_{a50}/h = 2.33 \times 10^{-17}$ m^3s^{-1}.

The log-deviation σ_{SD} of D_{eff} values is rather large compared to that quoted (0.45) for the failure time of the multi–interconnect structures in [7,8]; however the median Diffusivity value $D_{eff,50}$ itself is quite reasonable [e.g. 23]. In addition a second failure mode is quoted in [7,8] with a σ_{SD} value of 0.2 which acts to broaden the distribution, while here a single mode is assumed.

3.1. Growth time experiments [10–14] (jL^2)

The relationship between $L/MTTF$ and jL indicated by eqn (13) is now compared with the fixed length experimental observations of [11], Fig. (3). Close to j_{cr} only one term in the sum in eqn (11) is required so,

$$\frac{L}{t_f} \sim \frac{\pi^2 D}{4L \log\left(\frac{32}{\pi^3}\frac{j}{j - j_{cr}}\right)} \qquad (15)$$

With L = 50 μm and T = 300 K, as in [11], eqn (15) estimates a critical current density of 1.58×10^6 Acm^{-2}, while fitting eqn (4) produces a value of $j_{cr}L$ = 6319 Acm^{-1} (or $j_{cr} = 1.26 \times 10^6$ Acm^{-2}) thus underestimating j_{cr} by 25%. The result in [11] should probably, in any case, be presented as a critical jL^2 rather than critical jL.

Fig. (4) compares L^2/Dt_f from eqn (15) (solid curve and squares to provide 'data' points) as a function of j/j_{cr} together with $0.85*(j/j_{cr}–0.3)$ (dashed curve) and $1.05(j/j_{cr}–2/3)$ (dot–dashed curve). Fitting to large currents, underestimates the critical current by 70% while fitting to currents close to j_{cr} still underestimates j_{cr} by around 33%. This gives a useful comparison of the analysis in ref [12] which uses eqn (4) with $\bar{v}_{drift}$ from eqn (2) to obtain a plot of $1/t_f$ against j. Fig. 4 suggests such fits of 1/failure-time to the current may lead to a critical current in error by 25% or over.

The lognormal standard σ_{SD} deviation should not depend on $(j–j_{cr})$, eqn (14) as L decreases towards L_B. An increase in σ_{SD} as j approaches j_{cr} can be argued, but requires the development of the model with intra-line diffusivities – a shorter line averages over a smaller number of grains.

4. Conclusions

The purpose of this paper has been two fold. The

first is to investigate some potential misuses (eqns (3) and (4)) that are common in the analysis of critical length data. Such analysis requires the stress to rapidly reach a steady–state, and for the line to rupture, before the void starts to grow. The experimental support on which it is based relates to a rather different situation in Al(Cu) in which copper diffusion reaches a steady–state before the aluminium migration begins [18, 19].

The second purpose is to provide some analysis of short length data in DD Cu interconnect. The definition of L_B pivots on the approach to the steady–state stress within the interconnect. If the critical void size/rupture stress is reached before the steady–state is able to stop the atomic migration, the line will fail. *Any* line that ruptures will eventually fail as the stress gradient which would prevent void growth is relieved during the rupture. In copper it is generally believed that voids nucleate relatively quickly (n = 1 in the Black equation and this is borne out by most simulations e.g. [17 and references therein]. Close to L_B, the steady–state is reached exponentially slowly. It is the approach to the critical rupture stress/void size that is important in defining an immortal line, and hence L_B, and not the steady–state velocity of the void front afterwards (as in [5–8]. In addition an alternative analysis of the existing short length data can bring important information about failures and this may be used to corroborate EM models. For example, in this case, the probability of mortality within the time limit of the experiment is used to extract information on the cdf of the atomic diffusivity values. Finally, this work supports recent analysis which suggests that the variation of D_a values between grains is important to all EM analysis [e.g. 17].

References

[1] Korhonen MA, Børgesen P, et al. Stress evolution due to electromigration in confined metal lines, J. Appl. Phys. **73** (1993) 3790-3799.

[2] He J, Suo Z, et al., Electromigration lifetime and critical void volume. Appl. Phys. Letts., **85** (2004), 4639-4641.

[3] Oates AS and Lin MH, Void nucleation and growth contributions to the critical current density for failure of Cu vias, 47th IRPS Symp. **47** (2009) 452–457.

[4] Blech IA and Kinsbron E, Electromigration in thin solid gold films on Molybdenum surfaces. Thin Solid Films **25** (1975) 327 –334.

[5] Lee K–D, Ogawa ET, et al., Electromigration reliability of dual–damascene Cu/porous MSQ low k interconnects Appl. Phys. Letts. **82** (2003) 2032–2034.

[6] Lee K–D, Ogawa ET, et al., Electromigration critical length effect in Cu/oxide dual–damascene interconnects Appl. Phys. Letts. **79** (2001) 3236–3238.

[7] Ogawa ET, K–D Lee, et al., Electromigration reliability issues in dual–damascene Cu interconnects. IEEE Trans. Reliab. **51** (2002) 403–419.

[8] Ogawa ET, Bierwag AJ, et al., Direct observation of a critical length effect in dual–damascene Cu/oxide interconnects, Appl. Phys. Letts. **78** (2001) 2652–2654.

[9] Wang P–C, Filippi RG and Gignac LM, Electromigration threshold in single damascene copper interconnects with SiO_2 dielectrics. Proc Interconnect Tech (2001) 263–265.

[10] Wang P–C and Filippi RG. Electromigration threshold in copper interconnects. J Appl. Phys. **78** (2001) 3598-600.

[11] Lin MH, Lin MT and Wang T, Effects of length scaling on Electromigration in dual damascene copper interconnects. Microel. Reliab. **48** (2008) 569–577.

[12] Oates AS and Lin MH, Electromigration failure distribution of Cu/low–k dual–damascene vias: Impact of the critical current density and a new reliability extrapolation methodology. IEEE Trans. Dev. Mat. Reliab. **9** (2009) 244–254.

[13] Lin MH, Chang KP et al., Effects of width scaling and layout variation on dual damascene copper interconnect Electromigration. Microel. Reliab. **47** (2007) 2100–2108.

[14] Ney D, Federspiel X, et al., Stress induced Electro-migration backflow effect in copper interconnects IEEE Trans. Dev. Mat. Reliab. **6** (2006) 175–179.

[15] Choi Z–S, Mönig R and Thompson CV, Dependence of the electromigration flux on the crystallographic orientations of different grains in polycrystalline copper interconnects. Appl. Phys. Lett. **90**, 241913 (2007);

[16] Lloyd JR, Electromigration and Mechanical Stress, Microelectronic Engineering 49 (1999) 51-64

[17] Dwyer VM, An investigation of Electromigration induced void nucleation time statistics in short copper interconnects. J. Appl. Phys, **107** (2010) 103718.

[18] Wang P-C, Noyan IC, Kaldor SK, Jordan-Sweet JL, Liniger EG and Hu C-K, Real-time x-ray microbeam characterization of electromigration effects in Al.Cu. wires, Appl Phys Letts, **78**, (2001) 2712 – 2715.

[19] Wang P-C et al., Electromigration-induced stress in aluminium conductor lines measured by x-ray microdiffraction, Appl Phys Letts, **72**,(1998)1296– 1298.

[20] Hu C-K et al., Electromigration and stress-induced voiding in fine Al and Al-alloy thin film lines, IBM J Res Dev, **39**, (1995) 465 – 497.

[21] Hu C-K and R. Rosenberg R, Capping Layer Effects on Electromigration in Narrow Cu Lines, 7th International Workshop On Stress-Induced Phenomena In Metallization, AIP Conf. Proc. **741**, (2004) 97-111

[22] The Cu:SiN_x diffusion activation energy Q~0.9eV (ref [19]) while in Al(Cu) Q~0.7eV for Al, slowed down by the Al_2Cu precipitates. For the copper in the Al(Cu) grain boundary network Q should be considerably smaller [18].

[23] L Arnaud et al., Electromigration induced void kinetics in Cu interconnects for advanced CMOS nodes, Inter Rel Phys Sym (2011), 3E.1.1-3E.1.10, Monterey, CA, USA.